

# Bose-Einstein Condensates in Rotating Lattices

Rajiv Bhat, L. D. Carr\* and M. J. Holland

JILA, National Institute of Standards and Technology and Department of Physics, University of Colorado Boulder, CO 80309

(Dated: December 2, 2024)

Strongly interacting bosons in 2D in a rotating square lattice are investigated via a modified Bose-Hubbard Hamiltonian. Such a system corresponds to a rotating lattice potential imprinted on a trapped Bose-Einstein condensate. Second-order quantum phase transitions between the rotational ground states of the system, which reflect the underlying symmetry of the lattice unit cell, are described. A maximal phase winding of  $6\pi$  signifies a tightly-packed vortex lattice.

PACS numbers:

One of the most exciting recent advances in the field of ultracold quantum gases has been the realization of quantum phase transitions in Bose-Einstein condensates (BEC's) trapped in a lattice [1], in particular the superfluid to Mott insulator transition [2]. Quantum Phase Transitions typically occur when a topological change happens in the ground state symmetry as a function of a Hamiltonian parameter at zero temperature [3]. They play an important role in many models, including the quantum Ising model, quantum rotors, and the Bose-Hubbard model [3]. The latter very accurately describes experimental observations of the superfluid-Mott transition in BEC's [4, 5].

A second fruitful development in BEC's has been the study of rotating systems in harmonic traps, in which an Abrikosov lattice of quantized vortices appears for sufficient rotation [6]. Rotating BEC's have also been predicted to realize an analog of the fractional quantum Hall effect [7]. More generally, the density, temperature, lattice structure, and strength and symmetry of interactions in ultracold quantum gases are precisely and dynamically controllable in experiments, with no impurities or disorder. Thus these systems are accurately described by relatively simple model Hamiltonians. In this sense they are a playground for quantum many body theory.

In this Letter, we pull together these two cutting edge areas of study in BEC's, i.e., rotating systems and quantum phase transitions in lattices. Specifically, we derive and solve a modified Bose-Hubbard Hamiltonian for rotating BEC's trapped in a 2D square lattice potential with a filling factor. In addition to the superfluid-Mott transition, which can be driven by hopping and/or rotation, we find that a quantum phase transition occurs each time the total phase winding of the system increases by  $2\pi$ , up to a maximum value which depends on the rotational symmetry of the lattice unit cell and whether the center of rotation is peak-centered or valley-centered. In Fig. 1 is sketched one way to make a rotating lattice, as has already been experimentally realized at JILA [8]. Some theoretical aspects of this problem for large filling factors, such as vortex pinning [9] and structural phase transitions of vortex matter [10], have been studied previously. In contrast, we will consider filling factors of less

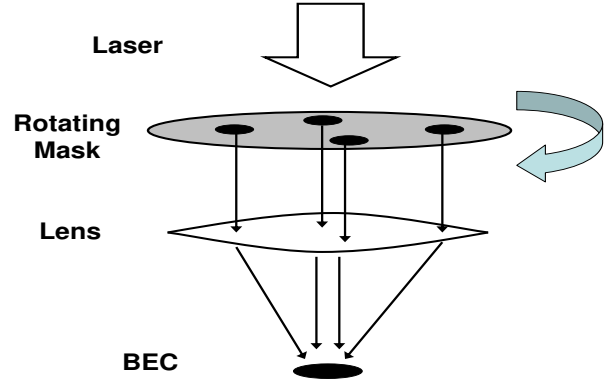


FIG. 1: (color online) Sketch of a rotating lattice. A laser beam passes through a rotating mask. A lens focuses the resulting lattice beam profile onto a stationary, trapped BEC. The lattice potential is imprinted via off-resonant interactions between the laser and the atoms.

than unity. In particular, we treat small, finite systems where exact solution via diagonalization of the Hamiltonian in a truncated Hilbert space is both insightful and correct. Our approach builds up a scalable picture of the lattice physics from the microscopic interaction and lattice structure.

Consider bosons in 2D, interacting via a two-body contact potential of strength  $g$  in a 2D lattice potential  $V^{\text{lat}}(x, y) = V^{\text{lat}}(x+jd, y+kd)$  which rotates about the  $z$  axis, where  $j, k$  are integers and  $d$  is the lattice constant. In the rotating frame the Hamiltonian is

$$\hat{H} = \int d^2r \hat{\Phi}^\dagger \left[ -\frac{\hbar^2}{2M} \nabla^2 + \frac{g}{2} \hat{\Phi}^\dagger \hat{\Phi} + V^{\text{lat}} - \Omega L_z \right] \hat{\Phi}, \quad (1)$$

$$L_z \equiv -i\hbar(x\partial_y - y\partial_x) \quad (2)$$

with rotation frequency  $\Omega$  and atomic mass  $M$ , where  $\hat{\Phi}^\dagger(x, y)$  and  $\hat{\Phi}(x, y)$  are field operators obeying the usual bosonic commutation relations. Using a Wannier basis, the operators can be expanded as a sum over bosonic field operators  $\hat{a}^\dagger, \hat{a}$ :

$$\hat{\Phi}^\dagger(x, y) = \sum_i \hat{a}_i^\dagger W_i^*(x, y). \quad (3)$$

The usual single-band Bose-Hubbard model [2, 3] is obtained via the tight binding and lowest band approximations [12]. A Gaussian of width  $\sigma$  is used for the lowest band Wannier basis:

$$W_i(x, y) = \exp\{-(x - x_i)^2 + (y - y_i)^2]/4\sigma^2\}/\sqrt{2\pi}\sigma, \quad (4)$$

where  $(x_i, y_i)$  are the coordinates of the  $i^{\text{th}}$  site. The rotational part  $\hat{H}_L \equiv \int d^2r \hat{\Phi}^\dagger \Omega L_z \hat{\Phi}$  of Eq. (1) becomes

$$\begin{aligned} \hat{H}_L &= -i\hbar\Omega \int d^2r \sum_{\langle i,j \rangle} \\ &\quad \left[ \hat{a}_j^\dagger \hat{a}_i (W_j^*(x, y) (x\partial_y - y\partial_x) W_i(x, y)) + \text{h.c.} \right] \\ &\equiv i\hbar\Omega \sum_{\langle i,j \rangle} K_{ij} (\hat{a}_i \hat{a}_j^\dagger - \hat{a}_i^\dagger \hat{a}_j), \end{aligned} \quad (5)$$

where  $\langle i, j \rangle$  indicates a sum over nearest neighbors. To obtain  $K_{ij}$ , we take  $\sigma = d/2$  and evaluate the integral for an infinite system [11]. Then

$$K_{ij} = (r_i r_j / ed^2) \sin \alpha_{ij}, \quad (6)$$

where  $r_i$  denotes the distance from the axis of rotation to the  $i^{\text{th}}$  site and  $\alpha_{ij}$  is the angle subtended by the  $i^{\text{th}}$  and the  $j^{\text{th}}$  sites with respect to the axis of rotation. Note that Eq. (6) is a purely geometrical, dimensionless factor.

Thus, the rotating Bose-Hubbard Hamiltonian is

$$\begin{aligned} \hat{H} &= -t \sum_{\langle i,j \rangle} (\hat{a}_i \hat{a}_j^\dagger + \hat{a}_j \hat{a}_i^\dagger) \\ &\quad - i\hbar\Omega \sum_{\langle i,j \rangle} K_{ij} (\hat{a}_i \hat{a}_j^\dagger - \hat{a}_j \hat{a}_i^\dagger) \\ &\quad + \frac{1}{2} U \sum_i \hat{n}_i (\hat{n}_i - 1) - \mu \sum_i \hat{n}_i, \end{aligned} \quad (7)$$

in the grand canonical ensemble. The hopping  $t$  and on-site interaction  $U$  have been explicitly calculated from  $g$ ,  $m$ , etc. elsewhere [12]. In Eq. (7) there is no phase winding superimposed onto the system, as was done by Wu *et. al* [13]. Equation (7) is the usual Bose-Hubbard Hamiltonian with the addition of the second term, which describes the rotating frame.

The expectation value of the current is an important observable in our analysis. In the Heisenberg picture the current is given by the Heisenberg equation of motion:

$$\begin{aligned} \langle \hat{J}_{ij} \rangle &= (i/\hbar d) \langle [\hat{n}_i, \hat{H}_{ij}] \rangle \\ &= \frac{it}{\hbar d} \langle \hat{a}_i \hat{a}_j^\dagger - \hat{a}_j \hat{a}_i^\dagger \rangle - \frac{\Omega K_{ij}}{d} \langle \hat{a}_i \hat{a}_j^\dagger + \hat{a}_j \hat{a}_i^\dagger \rangle, \end{aligned} \quad (8)$$

where  $\hat{H}_{ij}$  is the Hamiltonian for sites  $i, j$  alone. In Eq. (8), the first term is due to hopping while the second is due to current. Note that the sum over all nearest neighbors  $j$  of  $\langle \hat{J}_{ij} \rangle$  is zero, so that current is conserved in the rotating frame. Another useful observable is the total current on the lattice boundary  $C$ ,

$$\Lambda \equiv (\hbar d/E_r) \sum_{\langle i,j \rangle \in C} \langle \hat{J}_{ij} \rangle, \quad (9)$$

where we have scaled away the units via a “recoil” energy  $E_r \equiv \hbar^2/Md^2$  and all sums over  $C$  are taken with the

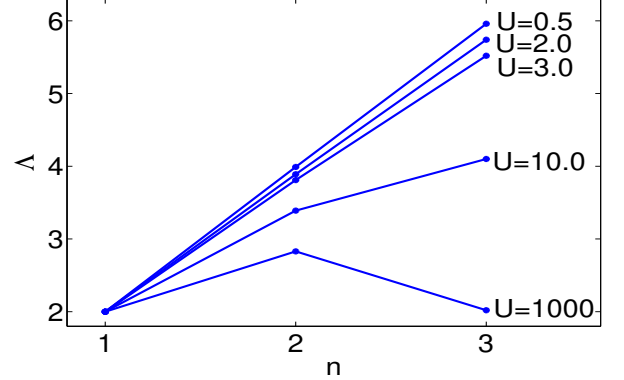


FIG. 2: (color online) The total dimensionless current  $\Lambda$  around a lattice unit cell is shown as a function of the average total number of atoms  $n$  in the system. The curves from top to bottom are for increasing on-site interaction strength  $U$  in units of the lattice recoil energy  $E_r$ . For weak interactions, the atoms behave independently; for strong interactions, there is a particle-hole symmetry, as evident in the bottommost curve, where  $n = 1$  and  $n = 3$  have the same  $\Lambda$ . The curves here are a guide to the eye.

same sign convention for helicity as  $\Omega$ . We also define two number-related observables:  $n = \sum_i \langle \hat{n}_i \rangle$ , the average total number of atoms in the system, and  $\nu \equiv \sum_i (\langle \hat{n}_i^2 \rangle - \langle \hat{n}_i \rangle^2) / \sum_i \langle \hat{n}_i \rangle$ , the normalized variance. Recall that  $\nu = 1$  for a coherent state,  $\nu > 1$  for a phase-squeezed state,  $\nu < 1$  for a number-squeezed state, and  $\nu = 0$  for a single Fock state.

For a Fock space consisting of only zero or one atoms per site, phase differences can be defined consistently. Suppose the ground state has one atom. Number conservation leads to a wavefunction of form

$$\begin{aligned} |\psi\rangle &= c_1 |1_1 0_2 \cdots 0_N\rangle + c_2 |0_1 1_2 \cdots 0_N\rangle \\ &\quad + \dots + c_N |0_1 0_2 \cdots 1_N\rangle, \end{aligned} \quad (10)$$

where subscripts within the kets are site indices and  $c_1, \dots, c_N$  are complex numbers, with  $N$  the total number of sites. Then the total phase winding on  $C$  is

$$\theta \equiv \sum_{\langle i,j \rangle \in C} \theta_{ij}, \quad \theta_{ij} \equiv [\arg(c_i) - \arg(c_j)], \quad (11)$$

which is  $2\pi$  times an integer value.

One can develop an algorithmic generalization of the definition of  $\theta$  in a consistent way for up to  $N$  total atoms in the system. For simplicity, we will focus our discussion on the strongly interacting case, achieved experimentally either by a Feshbach resonance or by turning up the lattice potential height to be very high, which reduces the hopping. In this case one can make a *two-state approximation* [14] which prevents multiple occupancy of the same site: this requires  $2^N$  kets as a basis of the many body system. Such a Fock space eliminates the interaction term  $U$  in Eq. (1). However, there are effective

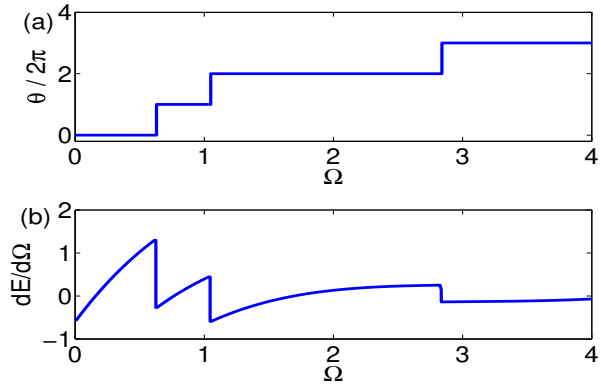


FIG. 3: (color online) (a) Phase winding around a  $4 \times 4$  lattice as a function of the rotation  $\Omega$  in units of  $E_r/\hbar$ , with total number of atoms  $n = 1$  and hopping  $t/E_r = 1$ . (b) The derivative of the ground state energy with respect to  $\Omega$ . The discontinuities indicate second order quantum phase transitions as each quantum of phase winding enters the system.

strong interactions due to atoms being unable to cross each other; i.e., one has a system of hard core bosons.

Having defined the observables, we first consider the case of a single square unit cell, i.e., a  $2 \times 2$ -site lattice. In order to assess the two-state approximation, we allow Fock states with up to three atoms per site: however, we keep the average number of particles per site at unity or below. We exactly diagonalize the Hamiltonian and find the ground state. Due to the competition between the hopping and rotational energy terms in Eq. (7), rotation enters the system only when  $\hbar\Omega > t$ . For an average *total* number of atoms  $n \in \{0, 1, 2, 3\}$ ,  $\theta = 0$  for  $\hbar\Omega < t$  and  $\theta = 2\pi$  for  $\hbar\Omega > t$ . For non-interacting atoms ( $U = 0$ ), this corresponds to  $\Lambda = 0$  and  $\Lambda = 2n$ , respectively. As the interatomic repulsion is increased,  $\Lambda$  decreases to non-integer values, as shown in Fig. 2. Although  $\theta$  is quantized,  $\Lambda$  is not. However, for  $t/U \ll 1$  and  $\hbar\Omega/U \ll 1$ , i.e., for very strong interactions, and/or a very strong lattice and small rotation, the allowed values of  $\Lambda$  return to those given by the two-state approximation. Thus, the two-state approximation is adequate to study strongly interacting systems.

Consider next a  $4 \times 4$ -site square 2D lattice, which consists of 9 unit cells. This is sufficient to describe a vortex lattice, as we will demonstrate. The two-state approximation is computationally necessary for exact diagonalization, so we study the strongly interacting case: *a priori* this is a  $2^{16}$ -ket basis. First, consider the simplified case of one atom in the system. Number conservation reduces the ground state to the simple form of Eq. (10). Numerical study of this case produces three main results. (1) Both the hopping  $t$  and the rotation  $\Omega$  can drive the system through a Mott-insulator/superfluid transition. (2) Second order quantum phase transitions occur each time a unit of total phase winding  $\theta$  enters the system. (3)

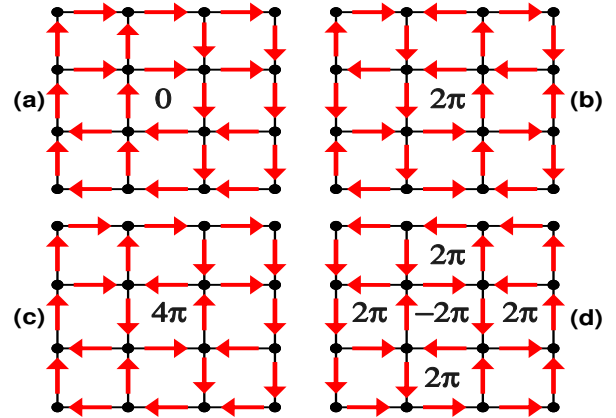


FIG. 4: (color online) The red arrows indicate direction of current flow for  $t/E_r = 1$  and  $n = 1$  at increasing rotations on a  $4 \times 4$  lattice, corresponding to phase windings of  $\theta = 0, 2\pi, 4\pi, 6\pi$ . (a)  $\hbar\Omega/E_r = 0.5$ ; (b)  $\hbar\Omega/E_r = 1.0$ ; (c)  $\hbar\Omega/E_r = 2.0$ ; (d)  $\hbar\Omega/E_r = 4.0$ . The last case is a vortex lattice.

The maximum  $\theta$  is  $6\pi$ .

Since rotation appears in Eq. (1) as a directional hopping, result (1) is not surprising. The Mott/superfluid transition has been extensively studied elsewhere [1, 2, 3, 4], so we do not discuss it further here. To illustrate result (2), in Fig. 3 is shown the total phase winding and the derivative of the total energy  $E \equiv \langle \hat{H} \rangle$  with respect to  $\Omega$ . Energy level crossings (not shown) are also observed, corresponding to each transition. The corresponding circulation patterns are shown in Fig. 4. In Fig. 4(a),  $\theta = 0$  and rotation has not yet entered the system. In the rotating frame, the current seems to be flowing backwards, i.e., clockwise. In Fig. 4(b),  $\theta = 2\pi$  and a single vortex enters the system and rests at the center. Figure 4(c) shows one of two possible patterns for  $\theta = 4\pi$ . Figure 4(d) is a tightly packed vortex lattice; the unit of negative vorticity at the center is a trivial result of packing four vortices together on a 2D square lattice.

Result (3) can be explained by breaking down  $\theta$  into a sum of phase windings around  $2 \times 2$  unit cells. The phase winding around the unit cell is mod  $8\pi$  since phase descriptions for phase windings  $\{0, 2\pi, 4\pi, 6\pi\}$  are indistinguishable from those for  $\{8\pi, -6\pi, -4\pi, -2\pi\}$ . Since  $\theta$  is a sum over unit cells, it is also mod  $8\pi$ . In general,  $\theta$  is mod  $(2m\pi)$ , where the lattice unit cell is  $m$ -fold symmetric. We have considered rotation centered on the peak of the lattice potential; for valley-centered rotation, as occurs for example in the  $3 \times 3$  case,  $\theta$  is mod  $(4m\pi)$ , and the smallest vortex contains multiple cells [15].

As in the case of the unit cell (see Fig. 2),  $\Lambda$  depends on the number of atoms and the strength of the interaction between them; it also depends on  $\theta$ . This latter dependence can be understood as follows. For one atom

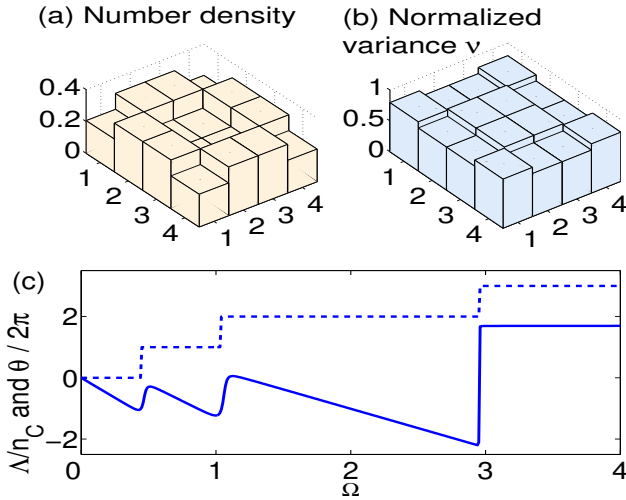


FIG. 5: (color online) Observables for a  $4 \times 4$  lattice with quarter-filling and  $t/E_r = 1$ . (a) Site-dependent number density  $n$  for  $\hbar\Omega/E_r = 1$ . There is noticeable depletion on the inner sites. (b) Site-dependent normalized variance  $\nu$  for  $\hbar\Omega/E_r = 1$ . Note that  $\nu < 1$ , so this is a number-squeezed ground state. (c) The normalized, scaled current  $\Lambda/n_C$  (solid curve) and the total phase winding (dashed curve), all on the boundary. Between each quantum phase transition, the normalized current depends linearly on the rotation  $\Omega$ .

in the system, from Eqs. (8)-(10),

$$\Lambda = \sum_C 2|c_i c_j| (t \sin \theta_{ij} - K_{ij} \hbar \Omega \cos \theta_{ij}) / E_r. \quad (12)$$

Since  $\theta_{ij}$  increases in discrete steps,  $\Lambda$  depends linearly on  $\Omega$  with a different slope for each phase winding. For  $\theta = 6\pi$  and 16 sites on  $C$ ,  $\theta_{ij} = \pi/2$  and the slope is zero. If one normalizes Eq. (12) to the total number of atoms on the boundary  $n_C \equiv \sum_{i \in C} \langle \hat{n}_i \rangle$ , the maximum value of  $\Lambda$  is exactly  $2t/E_r$ .

Finally, we extend our results to the case of general filling. The main difference from the single-atom case is the presence of effective strong interactions due to the use of the two-state approximation. In Fig. 5 are illustrated the number density  $n$ , normalized variance  $\nu$ , total phase winding  $\theta$ , and the normalized current on the boundary  $\Lambda/n_C$ , all for quarter filling. Note that  $n_C$  depends on  $\Omega$ . In Fig. 5(a)-(b) the site-dependence of  $n$  and  $\nu$  are illustrated for  $\hbar\Omega = t = E_r$ . In general, the density at the center varies for the same winding number, so that it is not an indication of vortex core size; in this strongly interacting system the core size is smaller than  $d$ . In Fig. 5(c) one observes that  $\Lambda$  depends linearly on  $\Omega$  between quantum phase transitions; this is qualitatively a similar result to that of one atom, as seen in Eq. (12). However,  $\max(\Lambda/n_C) \neq 2$ , due to interactions. The other essential features of general filling, i.e., the occurrence of quantum phase transitions and energy level crossings as units of phase winding enter the system, are qualitatively the same as that for one atom. This is a non-trivial result, as, in contrast to a single unit cell or a single atom on a  $4 \times 4$  lattice, general filling is not analytically tractable.

Finite-size effects make it difficult to use plots such as Fig. 3(b) to conclusively establish quantum phase transitions for a  $4 \times 4$  lattice. However, based on symmetry considerations, we identify transitions between rotational ground states as second order quantum phase transitions. As  $\Omega$  increases, the state of the system changes continuously while the phase winding, a symmetry-linked property, changes discontinuously. This fits with the definition of a second order phase transition [16]. First order phase transitions are usually not associated with changes in symmetry. Further, the system adopts higher rotational symmetries (1-fold, 2-fold and 4-fold) for higher rotational energy. This resembles the adoption of higher symmetry states at higher temperature seen in classical second order phase transitions. Finally, there is a small discrete set of total phase windings; this set is independent of the system size.

We note that the appearance of a vortex lattice in the discrete system should be observable by expansion and interference with a non-rotating system, as in the continuous case [6]. A second observable has been provided by our calculations: the current on the boundary jumps discontinuously with increasing  $\Omega$ . The maximal value of  $\Lambda$ , or, alternatively, a total phase winding of  $\theta = 6\pi$ , indicates the presence of a tightly packed vortex lattice.

We thank John Cooper, Meret Kraemer, Brian Seaman, and David Wood for useful discussions. We acknowledge the support of the Department of Energy, Office of Basic Energy Sciences via the Chemical Sciences, Geosciences and Biosciences Division.

---

[\*] Present address: Physics Department, Colorado School of Mines, Golden, CO 80401

[1] M. Greiner *et al.*, Nature **415**, 39 (2002).

[2] M. P. A. Fisher *et al.*, Phys. Rev. B **40**, 546 (1989).

[3] S. Sachdev, *Quantum Phase Transitions* (Cambridge University Press, New York, 1999).

[4] D. Jaksch, C. Bruder, J. I. Cirac, C. W. Gardiner, and P. Zoller, Phys. Rev. Lett. **81**, 3108 (1998).

[5] M. Greiner, O. Mandel, T. Hansch, and I. Bloch, Nature **419**, 51 (2002).

[6] K. W. Madison *et al.*, Phys. Rev. Lett. **84**, 806 (2000); J. R. Abo-Shaeer *et al.*, Science **292**, 476 (2001); P. C. Haljan *et al.*, Phys. Rev. Lett. **87**, 210403 (2001).

[7] N. K. Wilkin and J. M. F. Gunn, Phys. Rev. Lett. **84**, 000006 (2000); V. Schweikhard *et al.*, Phys. Rev. Lett. **92**, 040404 (2004).

[8] V. Schweikhard, private communication (2005).

[9] J. W. Reijnders and R. A. Duine, Phys. Rev. A **71**, 063607 (2005).

[10] H. Pu, L. O. Baksmaty, S. Yi, and N. P. Bigelow, Phys. Rev. Lett. **94**, 190401 (2005).

[11] For smaller lattices, the error due to the finite size introduces a small correction to the constant  $e$  in Eq. (6).

[12] A. M. Rey *et al.*, J. Phys. B: At. Mol. Opt. **36**, 825 (2003).

[13] C. Wu, *et al.*, Phys. Rev. A **69**, 043609 (2004).

- [14] L. D. Carr and M. J. Holland, Phys. Rev. A Rapid Communications, in press; e-print cond-mat/0501156 (2005).
- [15] R. Carretero-González *et al.*, Phys. Rev. Lett. **94**, 203901 (2005).
- [16] L. D. Landau and E. M. Lifshitz, *Statistical Physics* (Pergamon Press, New York, 1969).